See related commentary on pg 882

ORIGINAL ARTICLE

Fibronectin Peptides that Bind PDGF-BB Enhance Survival of Cells and Tissue under Stress

Fubao Lin[1], Jia Zhu[2], Marcia G. Tonnesen[3,4], Breena R. Taira[5], Steve A. McClain[6], Adam J. Singer[6] and Richard A.F. Clark[1,3]

Stressors after injury from a multitude of factors can lead to cell death. We have identified four fibronectin (FN) peptides: two from the first FN type III repeat ($FNIII_1$), one from the 13th FN type III repeat ($FNIII_{13}$), and one from FN variable region (IIICS), which when tethered to a surface acted as platelet-derived growth factor-BB (PDGF-BB) enhancers to promote cell survival. One of the $FNIII_1$ peptides and its smallest (14-mer) bioactive form (P12) were also active in solution. Specifically, P12 bound PDGF-BB ($K_D = 200$ nM), enhanced adult human dermal fibroblast (AHDF) survival under serum starvation, oxidative or endoplasmic reticulum stressors, and limited burn-injury progression in a rat hot comb model. Furthermore, P12 inhibited endoplasmic reticulum stress–induced c-Jun N-terminal kinase (JNK) activation. Although many growth factors have been found to bind FN directly or indirectly, here we identify peptide sequences of growth factor–binding sites in FN. The finding of these peptides further delineated how the extracellular matrix protein FN can support cell survival. As the peptide P12 is active in either soluble form or tethered to a substrate, it will have multifactorial uses as a bioactive peptide by itself or in tissue engineering.

Journal of Investigative Dermatology (2014) **134,** 1119–1127; doi:10.1038/jid.2013.420; published online 7 November 2013

INTRODUCTION

Tissue injury after stroke, heart attack, burns, or other trauma is a dynamic process that extends in size and severity over several days, leading to excess mortality and morbidity (Brait *et al.*, 2010; Shupp *et al.*, 2010; Piper and Garcia-Dorado, 2012). After injury, the central necrotic tissue is surrounded by ischemic, less severely affected tissue that potentially remains salvageable. However, as the ischemic tissue is exposed to various stresses such as nutrition depletion, reactive oxygen species (ROS), cytokines, and hypoxia, tissue cells in this region often die, by either apoptosis or necroptosis (Galluzzi and Kroemer, 2008; Lanier *et al.*, 2011; Hirth *et al.*, 2013), unless effective postinjury therapy is given (Yuan, 2009). Hence, preventing cell death in potentially salvageable tissue of an acutely damaged organ is a major goal for therapies of these injuries.

Fibronectin (FN) (Figure 1a), an extracellular protein found in blood and connective tissue, has a crucial role in cell growth, survival, migration, angiogenesis, and wound healing (Yamada and Clark, 1996). In the absence of tissue cell–derived FN, plasma FN can support neuronal survival and reduce brain injury following transient focal cerebral ischemia (Sakai *et al.*, 2001). Although FN probably supports cell survival in many ways, one mechanism is the interaction of RGD peptide in the 10th FN type III repeat ($FNIII_{10}$) with integrin receptors. For example, the FN integrin receptor α5β1 supports Chinese hamster ovary cell survival and upregulates Bcl-2 expression (Zhang *et al.*, 1995). In addition, FN-ligated α5β1 and αvβ3 integrins promote brain capillary endothelial cell survival and proliferation *via* mitogen-activated protein kinase signaling (Wang and Milner, 2006). FN-dependent survival signaling transits through phosphatidylinositide 3 kinase and NF-κB pathways in human bronchial epithelial cells (Han and Roman, 2006).

Platelet-derived growth factors (PDGFs) are major mitogens and survival factors for most mesenchymal cell types including fibroblasts (Romashkova and Makarov, 1999). PDGF occurs as five isoforms, classic PDGF-AA, AB, and BB isoforms, and the more recently described PDGF-CC and PDGF-DD isoforms (Fredriksson *et al.*, 2004). The most potent PDGF isoforms, -AB and -BB, are secreted either by platelets (PDGF-AB), macrophages (PDGF-BB), or epidermal cells (PDGF-BB) in response to injury. PDGFB knockout in mice is embryonic

[1]Department of Biomedical Engineering, Stony Brook University, Stony Brook, New York, USA; [2]Departments of Biochemistry and Cell Biology, Stony Brook University, Stony Brook, New York, USA; [3]Department of Dermatology, Stony Brook University, Stony Brook, New York, USA; [4]Department of Medicine, Northport VA Medical Center, Northport, New York, USA; [5]Olive View-UCLA Medical Center, Sylmar, California, USA and [6]Department of Emergency Medicine, Stony Brook University, Stony Brook, New York, USA

Correspondence: Richard A.F. Clark, Stony Brook University, HSC T16, 060, Stony Brook, New York 11794-8165, USA.
E-mail: richard.clark@stonybrook.edu

Abbreviations: AHDF, adult human dermal fibroblast; FN, fibronectin; FNIII, FN type III repeat; GFB, growth factor binding; GST, glutathione S-transferase; H_2O_2, hydrogen peroxide; HO/XO, hypoxanthine/xanthine oxidase; JNK, c-Jun N-terminal kinase; LC3, light chain 3; P1s, scrambled P1; PDGF, platelet-derived growth factor; p-JNK, phosphorylated JNK; ROS, reactive oxygen species; Tun, tunicamycin

Received 23 June 2013; revised 1 September 2013; accepted 12 September 2013; accepted article preview online 14 October 2013; published online 7 November 2013

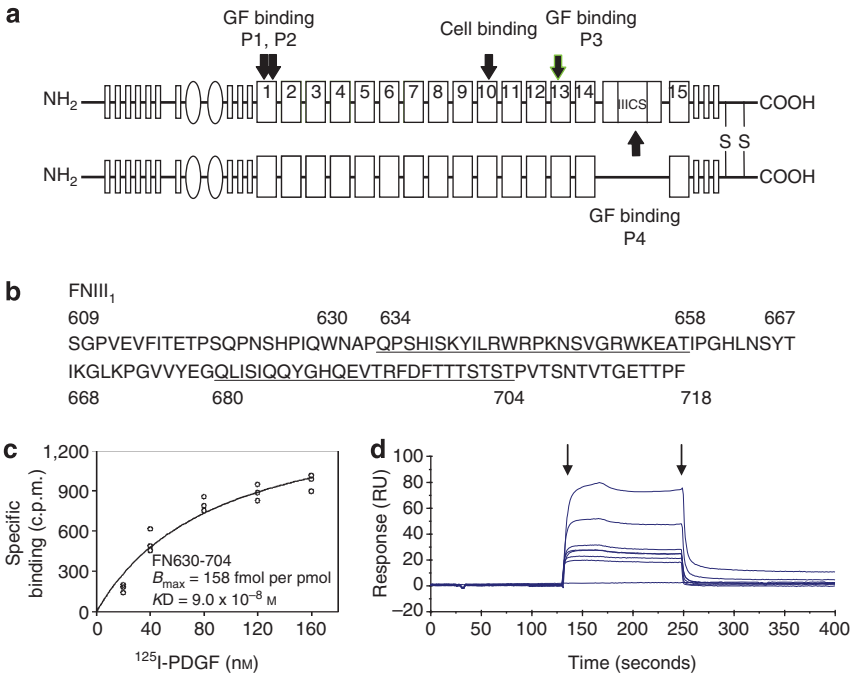

Figure 1. Peptide from first fibronectin type III repeat ($FNIII_1$) binds platelet-derived growth factor-BB (PDGF-BB). (**a**) Schematic of human FN. FN type I repeats are shown as thin rectangles, FN type II repeats as ovals, and FN type III repeats as thick rectangles. PDGF-BB and cell-binding sites are indicated (arrows). (**b**) Sequence of $FNIII_1$ (FN609-718). Sequences of P1 (FN634-658) and P2 (FN680-704) are underlined. (**c**) Equilibrium binding of PDGF-BB with anastellin (FN630-704). (**d**) Kinetic binding of PDGF-BB with FN630-704. Increasing concentrations (6.25–200 nM) of FN630-704 were injected across the biosensor chip coupled with PDGF-BB (first arrow), followed 120 seconds later by a continuing flow of buffer (second arrow). Chip without PDGF-BB was used as a reference. K_D was calculated by averaging the k_{off} divided by k_{on}. Sensorgrams are representative of three different experiments. c.p.m., counts per minute; RU, relative units.

lethal, whereas knockouts of other isoforms are not (Betsholtz, 2004).

Survival signals from FN and growth factors converge at the level of the focal contact (Plopper *et al.*, 1995) and are costimulatory (Miyamoto *et al.*, 1996) for progression through the cell cycle (Assoian and Schwartz, 2001). For example, FN can bind vascular endothelial growth factor and enhance its bioactivity (Wijelath *et al.*, 2006). It was more recently demonstrated that $FNIII_{12–14}$ bound a large number of growth factors (Martino and Hubbell, 2010) including PDGF-BB, which we confirmed (Lin *et al.*, 2011). Furthermore, we demonstrated that FN contains three growth factor–binding (FN-GFB) domains, i.e., $FNIII_1$, $FNIII_{13}$, and IIICS, respectively, which worked cooperatively with PDGF-BB to sustain optimal cell metabolism and prevent autophagy and apoptosis (Lin *et al.*, 2011). Here we identify four peptide sequences within these domains that bind PDGF-BB. In doing so, we discovered a 14-mer peptide that bound PDGF-BB and promoted cell survival, whether bound to a surface or presented to cells in fluid phase. Attributes of these FN-GFB peptides have important implications in tissue engineering.

RESULTS

First FNIII has two PDGF–binding sites

To define peptide sequences that bind PDGF-BB and support cell survival in FN-GFB domains (Lin *et al.*, 2011), we first focused on the first type III repeat of FN ($FNIII_1$)(Figure 1b) because the bioactive peptide, anastellin (FN630-704), resides within this domain and has been reported to promote FN fibrillogenesis (Ohashi and Erickson, 2005) and antitumor activity (Yi and Ruoslahti, 2001). To study whether anastellin interacted with PDGF-BB (^{125}I-labeled), anastellin was expressed with a cysteine (Cys) tag at the C terminus for sulfhydryl coupling to SulfoLink beads. From equilibrium-binding assays, anastellin–PDGF-BB interaction gave a K_D of 90 nM (Figure 1c). This finding was confirmed by kinetic-binding assays using plasmon surface resonance (Figure 1d; $K_D = 22.9$ nM).

To determine which peptide sequence(s) within anastellin bind(s) PDGF-BB, FN630-667 and FN668-704, representing the first and second halves of anastellin, were synthesized with Cys at their C termini. ELISA equilibrium-binding assays demonstrated that PDGF-BB bound FN630-667 with a K_D of 210 nM and FN668-704 with a K_D of 80 nM. Plasmon surface resonance confirmed binding of PDGF-BB to FN630-667 and FN668-704 (Supplementary Figure S1 online). These results demonstrated that $FNIII_1$ contains two PDGF-BB-binding sequences. Although it was known that $FNIII_1$ domain bound PDGF-BB (Lin *et al.*, 2011), the finding of two growth factor–binding sequences in this domain was a surprise.

Four peptides from three FN-GFB domains bound PDGF-BB

To determine whether similar peptide sequences existed in the two halves of anastellin, the two halves were analyzed by the PRATT software (Swiss Institute of Bioinformatics, Lausanne, Switzerland), a program that interactively generates

conserved patterns from a series of unaligned proteins. Two sequences—FN634-658 (QPSHISKYILRWRPKNSVGRWKEAT) from the first half of anastellin and FN680-704 (QLISHQQYG HQEVTRFDFTTTSTST) from the second half of anastellin—were found, and designated P1 and P2 (Supplementary Figure S2a online), respectively. To study whether these two 25-amino-acid peptides interacted with PDGF-BB, peptides were synthesized with a Cys at the C terminus for coupling to SulfoLink beads. ELISA equilibrium-binding assay using ^{125}I-PDGF-BB showed P1 and P2 binding with K_Ds of 250 and 110 nM, respectively (Supplementary Figure S2b and c). Interestingly, the P1 binding data fit a sigmoid binding curve (Supplementary Figure S2f online) better than the classic hyperbola curve shown in Supplementary Figure S2b online. The sigmoid curve had a Hills coefficient of 1.38, indicating modest cooperative binding between two sites. As PDGF-BB is an antiparallel homodimer, these data suggested that P1 binds both ends in a cooperative manner.

Next, we searched for other growth factor–binding sequences in FN, as well as all other proteins in the human proteome database using ScanProsite (Swiss Institute of Bioinformatics), a program that scans a sequence against PROSITE or a pattern against the UniProt Knowledgebase (Swiss-Prot and TrEMBL). Peptide sequences with similar patterns were found within $FNIII_{13}$ and IIICS, two domains that we previously reported had PDGF-BB-binding activity (Lin *et al.*, 2011). These two FN peptides were designated P3 (FN1853-1877) and P4 (FN2043-2076), respectively (Supplementary Figure S2a online). Equilibrium-binding assays with Cys-tagged P3 and P4 demonstrated that ^{125}I-PDGF-BB bound P3 and P4 with a K_D of 87 and 56 nM, respectively (Supplementary Figure S2d and e online). Thus, four PDGF-BB-binding peptides with similar sequence patterns were found within the three FN-GFB domains. Furthermore, a fifth similar sequence with growth factor–binding activity was found in the provisional matrix protein, vitronectin, but none other in the entire human proteome database.

FN-GFB peptides coupled to CBD/14 supports survival and decreases autophagy and apoptosis of FN-null cells in the presence of PDGF-BB

Previously, we showed that FN cell–binding domain ($FNIII_{8–11}$) did not support FN-null fibroblast survival in the presence of 1 nM PDGF-BB without the presence of a FN-GFB domain, i.e., $FNIII_1$, $FNIII_{13}$, or IIICS (Lin *et al.*, 2011). $FNIII_{8-11}$ (cell-binding domain) fused to the FN 14th type III repeat (CBD/14) has been reported to prevent cell spreading, thereby inducing anoikis and apoptosis (Dai *et al.*, 2005). However, CBD/14 in the presence either of $FNIII_1$, $FNIII_{13}$, or IIICS promoted optimal FN-null cell survival and response to PDGF-BB; the results are similar to those shown previously (Lin *et al.*, 2011). This finding led us to investigate whether FN-GFB peptides when coupled to CBD/14 supported FN-null cell survival. To address this question, cell survival assays were carried out in serum-free medium on wells precoated with FN or with glutathione *S*-transferase (GST)-CBD/14 fusion product ± tethered FN-GFB peptides. As shown previously, GST markedly improves protein adsorption to tissue culture plate surfaces (Lin *et al.*, 2011). Results showed that FN-null cells could not survive on CBD/14 even in the presence of PDGF-BB (Figure 2a). When cultured in serum-free DMEM plus 1 nM PDGF-BB, cells survived on surfaces precoated with CBD/14

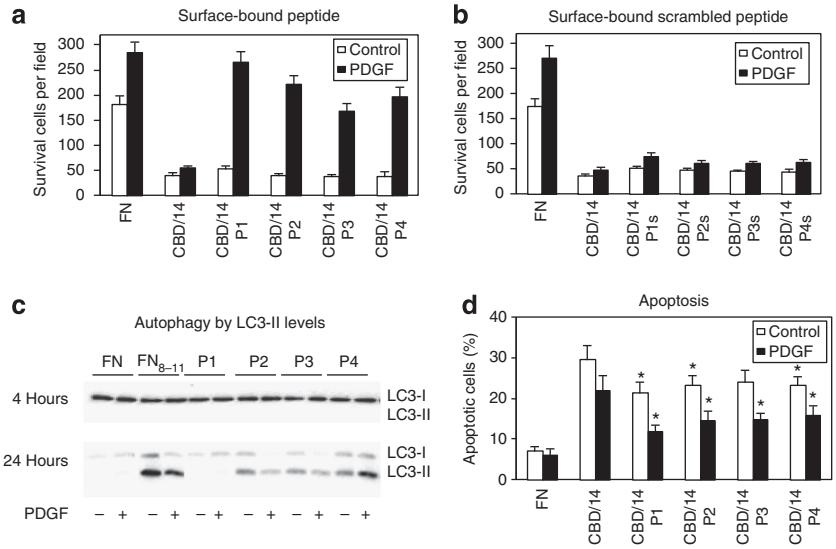

Figure 2. Fibronectin-growth factor binding (FN-GFB) peptide coupled to CBD/14 (cell-binding domain fused to the FN 14th type III repeat) supported FN-null fibroblast responsiveness to platelet-derived growth factor-BB (PDGF-BB). Cells were plated in 96-well (**a**, **b** and **d**) or 6-well (**c**) plates precoated with 0.125 μM FN or glutathione *S*-transferase (GST)-tagged CBD/14 ± tethered peptide and cultured in serum-free DMEM ± PDGF-BB at 37 °C for 3 days. (**a** and **b**) Viable cells in five × 10 fields were counted in three wells at 3 days (mean ± SD, $n = 15$). (**c**) Light chain 3-II (LC3-II) was detected by a size shift on western blot using a polyclonal antibody specific for LC3. (**d**) Apoptosis was determined by TUNEL at 3 days. Percent apoptosis was calculated from (positive cells per total cells) × 100. Fifty cells were counted in three replicate plates. Data points indicate mean ± SD. Each panel represents at least three experiments. *$P < 0.05$ compared with CBD/14. P1s, scrambled P1.

coupled to any one of the four FN-GFB peptides (Figure 2a), but did not survive on CBD/14 coupled to scrambled peptides (Figure 2b). Cell attachment was similar under all conditions (Supplementary Figure S3a online). Not surprisingly, FN-null cell metabolism was robust on FN, mediocre on CBD/14 even in the presence of PDGF-BB, but almost equivalent to FN when FN-GFB peptides were coupled to CBD/14 and cultured with PDGF-BB (Supplementary Figure S3b online).

FN-null cells cultured on FN-CBD/14 increased autophagy at 24 hours compared with those growing on FN even in the presence of PDGF-BB, as judged by quantification of total cellular light chain 3 (LC3), an inducible autophagosome component (Supplementary Figure S3c online), and western blot analysis for LC3-II, a cleaved LC3 product that is bound to autophagosomes (Figure 2c) (Klionsky *et al.*, 2012). When CBD/14 was coupled to FN-GFB peptides, the accumulations of LC3 or LC3-II in FN-null cells were significantly decreased (Supplementary Figure S3b and Figure 2c online, respectively). Thus, PDGF-BB could decrease autophagy in FN-null cells when plated on CBD/14 coupled to FN-GFB peptides, but not in cells on CBD/14 alone. This led us to investigate whether FN-GFB peptides also promoted the ability of PDGF-BB to limit apoptosis in FN-null cells cultured on CBD/14. FN-null cells showed little apoptosis up to 24 hours in all conditions (data not shown). FN-null cells cultured on FN showed low levels of apoptosis at 3 days, even in the absence of PDGF-BB (~7%), whereas PDGF-BB failed to prevent apoptosis in FN-null cells plated on CBD/14 (30% apoptosis at 3 days without PDGF-BB; 23% apoptosis with PDGF-BB) (Figure 2d). When FN-null cells were plated on CBD/14 coupled with a FN-GFB peptide, apoptosis was significantly decreased in the presence of PDGF-BB (Figure 2d).

Only P1 inhibited PDGF-BB binding to FN and FN-GFB domains

Next, we studied whether soluble FN-GFB peptides inhibited PDGF-BB binding to FN or FN-GFB domains ($FNIII_1$, $FNIII_{13}$, or IIICS). Binding assays of ^{125}I-PDGF-BB to FN or FN-GFB domains were carried out in the presence of FN-GFB peptides at various concentrations. At 4 μM, P1 inhibited over 75% binding of PDGF-BB to FN, and at 40 μM, the binding was nearly completely inhibited (Figure 3a). Scrambled P1 (P1s), with the same amino-acid composition and molar concentrations as P1, failed to inhibit PDGF-BB binding to FN (Figure 3a). Authentic P1 also inhibited PDGF-BB binding to $FNIII_1$, which contains P1 sequences (Figure 3b), as well as PDGF-BB binding to the other FN-GFB domains. Specifically, P1 inhibited PDGF-BB binding to $FNIII_{12–14}$ and IIICs in a concentration-dependent manner (Figure 3c and d, respectively). At 40 μM, P1 inhibited nearly all the binding of PDGF to these domains. In contrast, P1s showed no inhibition of PDGF-BB binding to FN or any FN-GFB domain (Figure 3b–d). Surprisingly, P2, P3, and P4 also failed to inhibit PDGF-BB binding to FN (Figure 3a) or any FN-GFB domain, even their parent domain (Figure 3b–d).

The ability of P1 to inhibit PDGF-BB binding to FN and to the three FN-GFB domains was not surprising, as FN-GFB peptides within these domains shared a similar sequence pattern. Furthermore, P1, when added in solution, significantly enhanced the survival of FN-null cells on CBD/14 in the presence of PDGF-BB (Figure 3e). Similar results were found for the survival of adult human dermal fibroblasts (AHDFs) growing in serum-deprived medium for 6 days (Figure 3f). Consistent with the lack of effect on FN-null cell survival, P2, P3, and P4 showed little effect on AHDF survival even in the presence of PDGF-BB (Figure 3f). Taken together, the inhibition experiments and the experiments with individual FN-GFB peptides in solution demonstrated that P1 had special growth factor–binding properties, such as cooperative binding shown in Supplementary Figure S2f online, which potentiated its ability to promote cell survival.

P12 is the shortest FN-derived peptide to enhance FN-null cell survival

To determine the minimal amino-acid sequence that enhanced cell survival, we investigated whether P11, a 20-residue peptide from the first third of anastellin that terminates after RWRPK, a vasoactive peptide described by the Hocking group (Hocking *et al.*, 2008), had PDGF-BB-binding and FN-null cell survival activity (Supplementary Table S1 online). P11 and P5, which overlap with P1 and P11, bound PDGF-BB and promoted PDGF-BB survival signals (Supplementary Table S1 online). Next, a series of peptides were obtained by progressively trimming P5, starting from either N or C termini (Supplementary Table S2 online), and were tested for bioactivity. Only P12, a peptide with one residue deletion from the N terminus of P5, supported FN-null cell survival in the presence of PDGF-BB (Supplementary Figure S4a online) and inhibited PDGF-BB binding to FN (Supplementary Figure S4b online). Real-time binding studies showed that P12 interacted with PDGF-BB with a K_D of 200 nM, and tissue culture investigations demonstrated that P12 could collaborate with PDGF-BB to enhance AHDF survival in serum-free medium (Supplementary Figure S5 online). These results demonstrated that P12, a 14-mer peptide, was the smallest peptide with P1 activity.

P12 enhanced AHDF survival under stress conditions

The unique ability of soluble P12 to enhance FN-null cell survival led us to investigate whether P12 could also enhance tissue cell survival under stress conditions. AHDFs were challenged with ROS stress or endoplasmic reticulum stress. AHDFs in the presence of serum were challenged with hypoxanthine/xanthine oxidase (HO/XO) or hydrogen peroxide (H_2O_2). The HO/XO system generates constant low levels of ROS, whereas H_2O_2 is a bolus ROS insult. AHDFs were sensitive to both HO/XO (Supplementary Figure S6a online) and H_2O_2 (Supplementary Figure S6b online). In the HO/XO system, cell death was inhibited when P12 was introduced 20 hours earlier or at the same time with oxidative stress. With H_2O_2, P12 only showed protective effect on AHDF survival when AHDFs were preincubated with P12 before H_2O_2 challenge. P12 in the presence of PDGF-BB or serum also promoted cell survival when endoplasmic reticulum stress was induced by tunicamycin (Tun), as judged by the XTT (2,3-bis-(2-methoxy-4-nitro-5-sulfophenyl)-2*H*-tetrazolium-5-carboxanilide) assay (Figure 4).

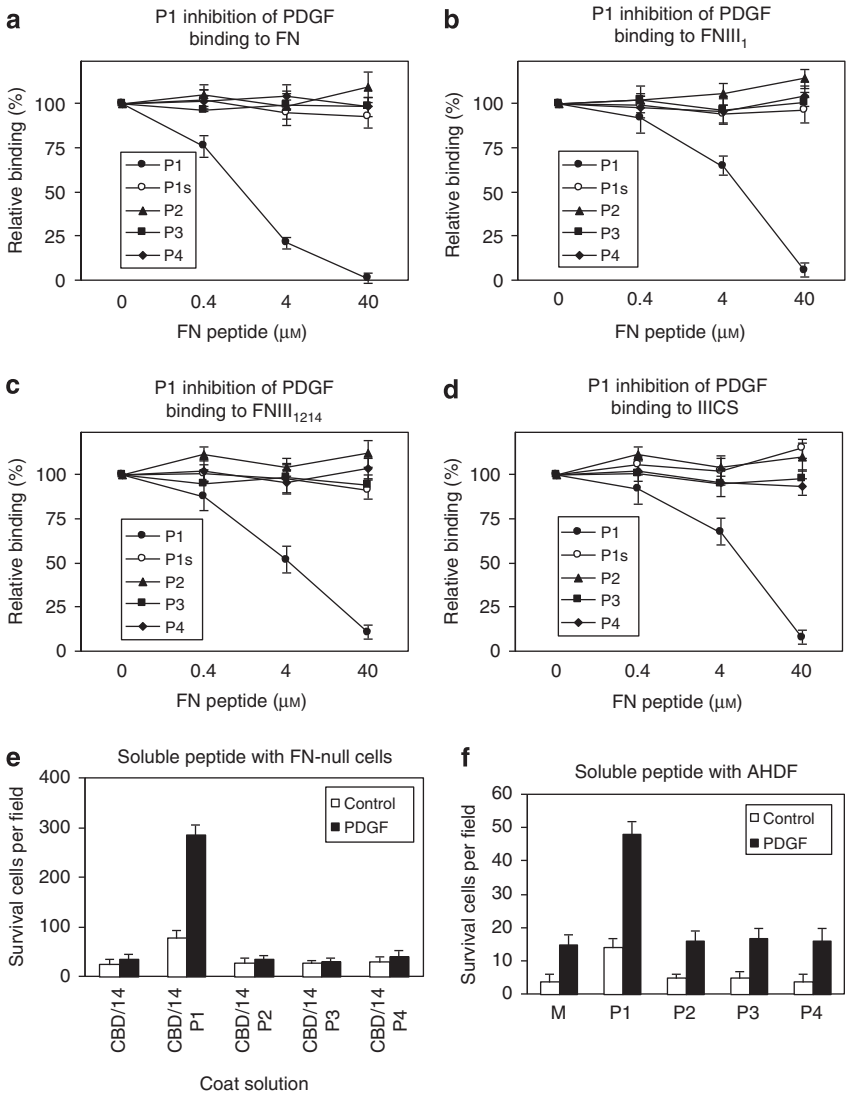

Figure 3. Soluble P1 inhibited platelet-derived growth factor-BB (PDGF-BB) binding to fibronectin (FN) and FN-growth factor binding (FN-GFB) domains, and supported FN-null cell and adult human dermal fibroblast (AHDF) survival. (**a**–**d**) ^{125}I-radiolabeled PDGF-BB was incubated with FN or glutathione *S*-transferase (GST)-tagged FN-GFB domain-coated wells. After washing, radioactivity of bound PDGF-BB was determined using a γ-counter. (**e**) Fluid-phase P1 supported FN-null cell survival on CBD/14 (cell-binding domain fused to the FN 14th type III repeat). FN-null fibroblasts were plated at 4,000 cells per well (96-well-plates) precoated with 0.125 μM GST-tagged CBD/14 in serum-free DMEM ± 1 nM PDGF-BB ± 10 μM peptide at 37 °C for 3 days. Viable cells in five × 10 fields were counted in three wells (mean ± SD, $n = 15$). (**f**) Fluid-phase P1 supported AHDF survival under serum-starvation conditions. AHDFs were plated at 1,000 cells per well (96-well plates) in serum-free DMEM and cultured overnight, and then changed to DMEM ± 1 nM PDGF-BB ± 10 μM peptide was added, cells were cultured for 6 days, and viable cells were counted. Data shown are mean ± SE ($n = 4$).

As endoplasmic reticulum stress is coupled to Jun N-terminal kinase (JNK) activation (Urano *et al.*, 2000), which can lead to cell death by apoptosis (Urano *et al.*, 2000; Lin *et al.*, personal communication), P12 effects on (JNKs) activation were investigated. After AHDFs were exposed to Tun in the presence of PDGF-BB ± P12 or P12s, phosphorylated JNK (p-JNK) was determined by immunoblotting (Figure 4a and b). In the presence of 1 nM PDGF-BB, but in the absence of P12, Tun significantly increased p-JNK by 4 hours. However, in the presence of both PDGF-BB and P12, p-JNK induction was markedly inhibited, whereas P12s showed a minimal effect.

P12 limited burn-injury progression in a rat hot comb model

The effect of P12 on burn-injury progression was assessed in a rat hot comb burn model, as described in the Materials and Methods section and in our previous publication (Singer *et al.*, 2011). Each hot comb contained four brass prongs that left three 5-mm non-burned interspaces. Burn-injury progression across the interspaces was assessed both visually and histologically. When P12 was infused 1 hour after burns, injury progression into the interspaces between burns was inhibited in a dose–response manner (Figure 5).

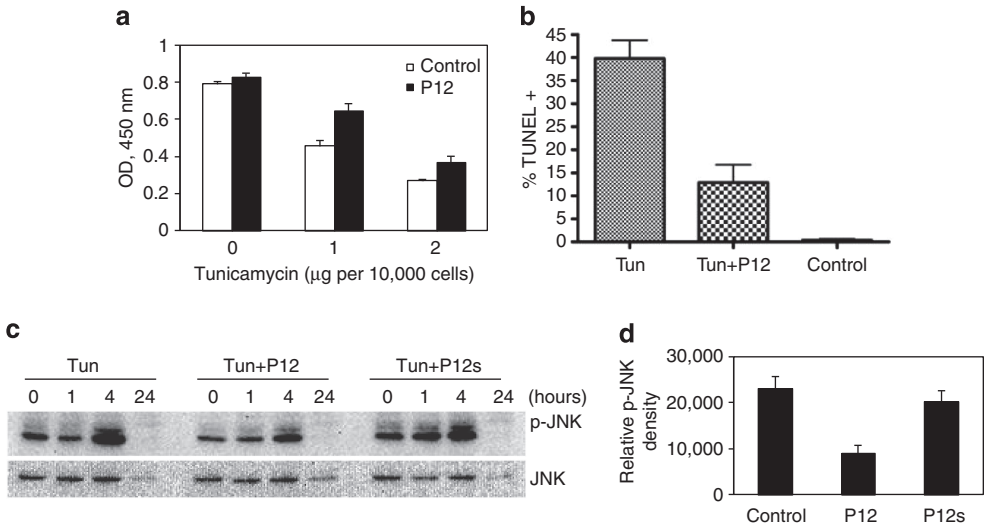

Figure 4. P12 enhanced adult human dermal fibroblast (AHDF) survival under tunicamycin (Tun)-induced endoplasmic reticulum stress and suppressed Tun-induced c-Jun N-terminal kinase (JNK) activation. (**a**) AHDFs at 1,000 cells per well were cultured in serum-free DMEM ± 1 nM platelet-derived growth factor-BB (PDGF-BB) in 96-well plates overnight and challenged with Tun at 1 or 2 μg per 10^4 cells for 4 hours. Cell viability was determined by XTT (2,3-bis-(2-methoxy-4-nitro-5-sulfophenyl)-2*H*-tetrazolium-5-carboxanilide) assay. Histograms show mean ± SD, $n = 4$. (**b**) AHDFs were incubated in serum-free DMEM + 1 nM PDGF-BB with 1 μg of Tun per 10^4cells ± 10 μM P12 for 20 hours. Apoptosis was determined by TUNEL assay. (**c** and **d**) AHDFs were cultured in complete DMEM and exposed to 5 μg ml^{-1} Tun (1 μg per 10^4 cells) ± 10 μM P12 or 10 μM scrambled P12 (P12s) for the indicated times. (**c**) Phosphorylated-JNK (p-JNK) levels were determined by immunoblotting. (**d**) Quantitative analysis of p-JNK band at 4 hours from three immunoblots, mean ± SD. OD, optical density.

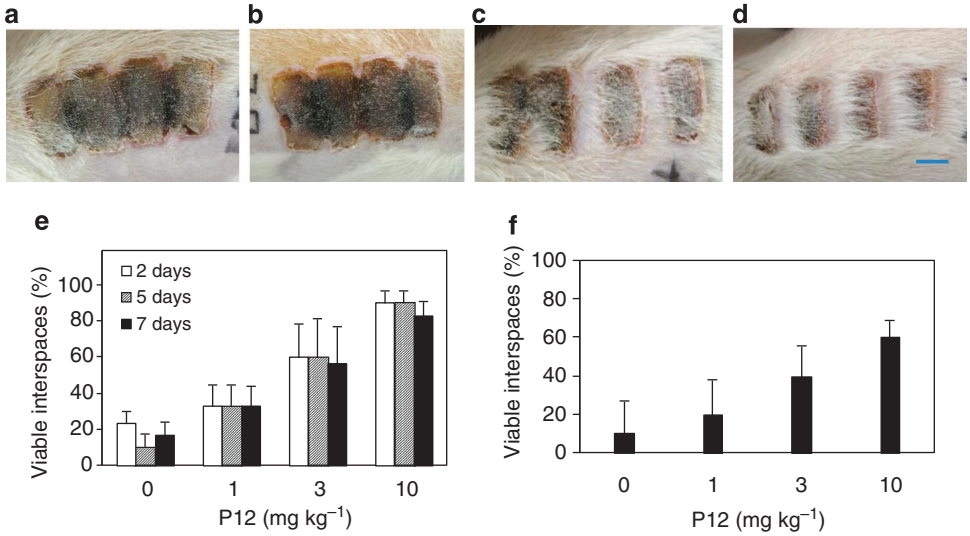

Figure 5. P12 intravenous infusion 1 and 24 hours after burn inhibited injury progression. (**a** and **b**) Burn at 7 days after injury without treatment. (**c** and **d**) Burn at 7 days after injury that had been treated with 10 mg kg^{-1} P12. (**e**) Viable interspaces 2, 5, and 7 days after injury in rats treated or not treated with P12. (**f**) Viable interspaces 7 days after injury determined by histologic analysis. 0 = Infusion with lactated Ringer's buffer. Variance of interspace viability among rats within a specific treatment arm was no more than variance among interspaces on a given rat; therefore, interspace data for all five rats per treatment arm were pooled; $n = 30$ interspaces (6 interspaces per rat) in five rats per treatment arm. Bar = 10 mm.

DISCUSSION

From our results, P12, a peptide from the first type III repeat of FN, appeared to act as a cofactor of PDGF-BB, enhancing its ability to promote survival of cells under stress. In addition, we found a similar peptide in vitronectin (Lin and Clark, unpublished data). Although it was previously established by us (Lin *et al.*, 2011) and others (Wijelath *et al.*, 2006; Martino and Hubbell, 2010) that FN can directly bind growth factors, and thereby enhance their activity, this is the first report that localized growth factor–binding and –enhancing activity to specific peptides within FN domains. We propose naming this new class of bioactive peptides that act as cofactors of growth

factors, particularly promoting their cell survival activity, epiviosamines from the Greek word *epivios*, the adjective of the verb epiviono, which means ''to survive in the face of adversity.'' The prefix *epivios* has been combined with ''amine,'' used to indicate a substance made from peptides. Historically, *vita*, the Latin word for life, was combined with amine to make the word vitamin for the same reason. However, when it was discovered that vitamins were not peptides, the ''e,'' from amine, was dropped.

Interestingly, the FN peptide P12, which had the most robust PDGF-BB-binding activity and which was active in solution, was found within the amino terminus of anastellin, a 76-mer peptide that promotes FN fibrillogenesis (Ohashi and Erickson, 2005), inhibits endothelial cell growth, and has antiangiogenesis activity (Yi and Ruoslahti, 2001). Preliminary investigations of P12 bioactivity on human dermal microvascular endothelial cells demonstrated that P12 did not inhibit human dermal microvascular endothelial cell metabolism when the cells were cultured with 10 ng ml^{-1} vascular endothelial growth factor in endothelial cell growth medium, whereas anastellin inhibited human dermal microvascular endothelial cells (McTigue M, Tonnesen MG and Clark RAF, unpublished observations). In contrast, fibroblast survival was not inhibited by anastellin in solution and was enhanced when anastellin was adsorbed on the culture dish. Furthermore, the carboxy terminus of P12 contains RWRPK, the carboxy terminus of vasoactive peptides previously described by the Hocking group (Hocking *et al.*, 2008). Although P12 has vasodilation activity on the microvascular bed of a hamster cheek pouch (Frame MD, Lin F and Clark RAF, personal communication), RWRPK does not collaborate with PDGF-BB to promote survival of FN-null cells. In fact, the Hocking group demonstrated that the RWRPK by itself inhibits cell growth (Hocking *et al.*, 2008). Thus, anastellin, P12, and RWRPK are nested peptides within the FN first type III repeat that have distinctly different biological activities.

The Hubbel group previously demonstrated that $FNIII_{12–14}$ bound a large number of growth factors (Martino and Hubbell, 2010) including PDGF-BB, as we confirmed (Lin *et al.*, 2011). Furthermore, we have confirmed that $FNIII_{12–14}$, as well as $FNIII_1$ and IIICS, bind multiple, but not all, growth factors. Often, only a few members of a growth factor family bind FN. From the differential binding of FN-GFB domains to growth factors, we have delineated peptide sequences within these growth factors to which P1, P2, P3, and P4 bind (Lin F and Clark RAF, personal communication). In fact, preliminary computer modeling done by Wallqist and Rollins at Ft Detrick, Frederick, MD, demonstrated a probable P12 docking site at the interface of PDGF-BB and the PDGF-BB receptor (PDGFR-β) that contains the putative PDGF-BB-binding partner peptide for P12. As there are two sites for P12 binding to the PDGF-BB antiparallel dimer, the cooperative binding pattern observed for P1 interaction with PDGF-BB is not surprising.

More recently, the Hubbell group demonstrated that multiple recombinant domains of FN, including the central cell-binding domain ($FNIII_{9–10}$) and the promiscuous $FNIII_{12–14}$ growth factor–binding domain, greatly enhanced the regenerative effects of growth factors in a diabetic mouse model and a critical-size rat bone defect (Martino *et al.*, 2011). In addition, the Hocking group recently demonstrated that FN recombinant fusion products consisting of the latter half of $FNIII_1$ fused to $FNIII_{8-10}$ enhanced wound healing in a diabetic mouse model (Roy *et al.*, 2013). Taken together, these two groups have used FN domains that contain three out of the four peptides that we have determined are the growth factor–binding sites in FN. The ability of P12 to limit burn-injury progression adds further evidence that FN growth factor–binding sites have utility in tissue survival and healing.

JNKs have a critical role in cell apoptosis initiated by both extrinsic and intrinsic pathways (Verma and Datta, 2012). To date, three JNKs, namely JNK1, JNK2, JNK3, encoded by three distinct genes have been identified (Johnson and Nakamura, 2007). In response to specific stimuli such as heat shock, reperfusion injury, ER, and oxidative stress, JNK proteins are activated by phosphorylation at its Thr or Tyr residues of a TXY motif. JNKs in turn activate apoptotic signaling either through the upregulation of pro-apoptotic genes *via* the transactivation of specific transcription factors including c-Jun or by directly modulating the activities of mitochondrial pro- and anti-apoptotic proteins through phosphorylation. Here we demonstrate that P12 promoted the ability PDGF-BB to suppress JNK activation. Therefore, the downregulation of the JNK pro-apoptotic pathway may be responsible in part for the decreased apoptosis observed of cells under stress that were treated with P12. The ability of P12 to limit burn-injury progression in a rat hot comb model is consistent with this hypothesis.

With elucidation of more epiviosamines such as P12, we will increase our understanding of how extracellular matrix proteins can enhance growth factor signaling in such a way to sustain cell survival in the setting of tissue stress (Macri *et al.*, 2007). In addition, the findings described here will increase the number of small peptide bioactives that can be added to tissue-engineered products to induce tissue survival and regeneration (Clark, 2013).

MATERIALS AND METHODS

Materials

Recombinant PDGF-BB was obtained from Biosource (Camarillo, CA) and ^{125}I-PDGF-BB from Amersham Biosciences (Piscataway, NJ). Human plasma FN was purchased from Chemicon (Temecula, CA) and found to be 99% pure and intact by SDS-PAGE. SulfoLink coupling beads was acquired from Pierce (Rockford, IL). Fatty acid–free BSA was purchased from ICN Biomedicals (Aurora, OH). Ni-NTA agarose beads were acquired from Qiagen (Valencia, CA). Isopropyl β-D-1-thiogalactopyranosideb and lysogeny broth were purchased from Fisher Scientific (Fair Lawn, NJ) and fetal bovine serum from Hyclone (Logan, UT). Culture plates were from BD Bioscience (Billerica, MA). The Cell proliferation kit II (XTT) was from Roche Diagnostics (Indianapolis, IN). LC3 polyclonal antibodies were from Santa Cruz Biotechnology (Santa Cruz, CA) and Novus Biologicals (Littleton, CO). BIAcore 2000, CM5 sensor chips, *N*-hydroxysuccinimide, *N*-ethyl-*N*′-(3-diethylaminopropyl)carbodiimide hydrochloride, and 1 M ethanolamine (pH 8.5) were purchased from BIAcore

(Piscataway, NJ). Peptides were synthesized by Bio-synthesis (Lewisville, TX) and PEGDVS was acquired from NEKTAR Transforming Therapeutics (Huntsville, AL).

Expression and purification of FN functional domains

Methods for cloning, expression, and purification of recombinant human FN domains and fusion products of FN domains with GST were published previously (Wang *et al.*, 2005). GST tag on the N terminus of the recombinant proteins facilitated FN domain adsorption onto tissue culture plastic for cell function studies. We also previously described cloning, expression, and purification of Cys-tagged FN domains (Ghosh *et al.*, 2006). Cys-tagged FN domains allowed linkage to SulfoLink agarose beads with minimal impact on protein conformation.

Equilibrium binding of PDGF-BB with FN or peptides

Cys-tagged FN peptides were conjugated to agarose beads *via* –SH groups, using the manufacturer's protocol (SulfoLink Coupling Gel). To block nonspecific binding, agarose beads, conjugated with or without FN or FN peptides, were incubated with 2% BSA at room temperature for 2 hours. For equilibrium binding, 20 µl of conjugated agarose beads were incubated with varying concentrations of ^{125}I-labeled PDGF-BB in binding buffer (DMEM + 1% BSA) at room temperature for 2 hours with rotation. After washing, the radioactivity bound to the agarose beads was quantified using a γ-counter. The binding constant of PDGF-BB with FN or FN domains was determined using Prism 4 nonlinear regression software (GraphPad, San Diego, CA).

Kinetic-binding assay of PDGF-BB with peptides

Using the BIAcore 2000 plasmon resonance system, kinetic binding constants were determined by passing varying concentrations of analytes dissolved in 20 mM HEPES, 150 mM NaCl, 3.4 mM EDTA, and 0.05% Tween-20, pH 7.4, over chip surfaces coupled with either PDGF-BB or purported FN-GFB partner, which were immobilized on the Sensor Chips as described previously (Lin *et al.*, 2011). All kinetic experiments were carried out at 20 °C at a flow rate of 30 µl minute^{-1}. For mass transport experiments, each analyte was injected at a fixed concentration and run at flow rates ranging from 5 to 75 µl minute^{-1}. All analytes were injected over a PDGF-coupled surface, as well as over a control surface for 120 s, followed by 300 s of dissociation in running buffer. Regeneration of the sensor chip for subsequent injections was accomplished by one pulse of 0.05% SDS (30 s). Sensorgrams were prepared and globally fitted using nonlinear least-squares analysis and numerical integration of differential rate equations following the BIAcore manual and using kinetic models available in BIAevaluation software (Biacore Life Science, Piscataway, NJ).

Cell culture

Mouse FN-null fibroblasts generated as described previously (Saoncella *et al.*, 1999) and AHDF (passages 5–13; Clonetics, San Diego, CA) were maintained in DMEM supplemented with 100 U ml^{-1} penicillin, 100 µg ml^{-1} streptomycin, and 10% fetal bovine serum at 37 °C and 5% CO_2/95% air in a humidified atmosphere. For cell function assays, fibroblasts were grown to approximately 80% confluence, harvested, and transferred to tissue culture plates in assay-appropriate numbers.

Mouse FN-null cell survival assays on FN domains

Cell survival experiments were performed in 96-well plates that had been coated with 0.125 µM of FN, CBD/14, or CBD/14 coupled with various peptides, as described previously (Lin *et al.*, 2011). After blocking with 2% BSA for 2 hours to exclude further protein binding, plates were washed with phosphate-buffered saline. For each well, 4,000 FN-null cells were plated and incubated at 37 °C for 4 hours. Next, 25 µl of 5% BSA in DMEM was added to each well ± PDGF-BB or FN peptides, and wells were incubated for the durations indicated. Cell survival was assayed by counting cells and by XTT according to the manufacturer's protocol.

TUNEL assay

Apoptotic cells were identified by nick end labeling using the *In Situ* Cell Death Detection Kit and TMR red, as described previously (Lin *et al.*, 2011).

Analysis of the autophagosome protein LC3

ELISA for total LC3 and western blots of LC3-I and LC3-II were performed as described previously (Lin *et al.*, 2011).

Rat hot comb burn model

Animal experiments were approved by the IACUC at Stony Brook University (Stony Brook, NY). Sprague–Dawley rats with a weight around 350 g were used. After removing hair, two burns were created on the back of each animal using a brass comb with four rectangular prongs preheated in boiling water and applied for 30 seconds, resulting in four rectangular 10 × 20 mm^2 full-thickness burns separated by three 5 × 20 mm^2 unburned interspaces (zone of ischemia). Forty comb burns with 120 unburned interspaces were created and distributed among control and three doses of P12 (1, 3, and 10 mg kg^{-1} administered in 1 ml of Lactated Ringer's solution). An observer blinded to the treatment determined necrotic interspaces at 2, 5, and 7 days. Full-thickness biopsies from interspaces 7 days after injury were processed, stained with hematoxylin and eosin, and evaluated for evidence of necrosis by a board-certified dermatopathologist (SAM) blinded to the protocol.

CONFLICT OF INTEREST

RAFC and FL codiscovered P12. RAFC is President and Founder of NeoMatrix Formulations, a biotechnology company engaged in preclinical studies for P12 treatment of burns. MGT is Secretary of NMF.

ACKNOWLEDGMENTS

This work was supported by NIH/NA10143 Merit Award (RAFC), NIH RC2 AR059384 (RAFC), and the Armed Forces Institute of Regenerative Medicine W81XWH-08-2-0034 (RAFC). We thank Deane F. Mosher for providing the FN-null cells.

SUPPLEMENTARY MATERIAL

Supplementary material is linked to the online version of the paper at http://www.nature.com/jid

REFERENCES

Assoian RK, Schwartz MA (2001) Coordinate signaling by integrins and receptor tyrosine kinases in the regulation of G1 phase cell-cycle progression. *Curr Opin Genet Dev* 11:48–53

Betsholtz C (2004) Insight into the physiological functions of PDGF through genetic studies in mice. *Cytokine Growth Factor Rev* 15:215–28

Brait VH, Jackman KA, Walduck AK *et al.* (2010) Mechanisms contributing to cerebral infarct size after stroke: gender, reperfusion, T lymphocytes, and Nox2-derived superoxide. *J Cereb Blood Flow Metab* 30: 1306–17

Clark RAF (2013) Wound repair: basic biology to tissue engineering. In: Lanza RP, Langer R, Chick WL eds *Principles of Tissue Engineering*. Elsevier: Amsterdam, Netherlands, Boston, MA, USA

Dai R, Iwama A, Wang S *et al.* (2005) Disease-associated fibronectin matrix fragments trigger anoikis of human primary ligament cells: p53 and c-myc are suppressed. *Apoptosis* 10:503–12

Fredriksson L, Li H, Eriksson U (2004) The PDGF family: four gene products form five dimeric isoforms. *Cytokine Growth Factor Rev* 15:197–204

Galluzzi L, Kroemer G (2008) Necroptosis: a specialized pathway of programmed necrosis. *Cell* 135:1161–3

Ghosh K, Ren XD, Shu XZ *et al.* (2006) Fibronectin functional domains coupled to hyaluronan stimulate adult human dermal fibroblast responses critical for wound healing. *Tissue Eng* 12:601–13

Han SW, Roman J (2006) Fibronectin induces cell proliferation and inhibits apoptosis in human bronchial epithelial cells: pro-oncogenic effects mediated by PI3-kinase and NF-kappa B. *Oncogene* 25:4341–9

Hirth DA, McClain SA, Singer AJ *et al.* (2013) Endothelial necrosis at 1 hour post-burn predicts progression of tissue injury. *Wound Repair Regen* 21:563–70

Hocking DC, Titus PA, Sumagin R *et al.* (2008) Extracellular matrix fibronectin mechanically couples skeletal muscle contraction with local vasodilation. *Circ Res* 102:372–9

Johnson GL, Nakamura K (2007) The c-jun kinase/stress-activated pathway: regulation, function and role in human disease. *Biochim Biophys Acta* 1773:1341–8

Klionsky DJ, Abdalla FC, Abeliovich H *et al.* (2012) Guidelines for the use and interpretation of assays for monitoring autophagy. *Autophagy* 8:445–544

Lanier ST, McClain SA, Lin F *et al.* (2011) Spatiotemporal progression of cell death in the zone of ischemia surrounding burns. *Wound Rep Regen* 19:622–32

Lin F, Ren XD, Pan Z *et al.* (2011) Fibronectin growth factor-binding domains are required for fibroblast survival. *J Invest Dermatol* 131:84–98

Macri L, Silverstein D, Clark RAF (2007) Growth factor binding to the pericellular matrix and its importance in tissue engineering. *Adv Drug Deliv Rev* 59:1366–81

Martino MM, Hubbell JA (2010) The 12th–14th type III repeats of fibronectin function as a highly promiscuous growth factor-binding domain. *FASEB J* 24:4711–21

Martino MM, Tortelli F, Mochizuki M *et al.* (2011) Engineering the growth factor microenvironment with fibronectin domains to promote wound and bone tissue healing. *Sci Transl Med* 3:100ra189

Miyamoto S, Teramoto H, Gutkind JS *et al.* (1996) Integrins can collaborate with growth factors for phosphorylation of receptor tyrosine kinases and MAP kinase activation: roles of integrin aggregation and occupancy of receptors. *J Cell Biol* 135:1633–42

Ohashi T, Erickson HP (2005) Domain unfolding plays a role in superfibronectin formation. *J Biol Chem* 280:39143–51

Piper HM, Garcia-Dorado D (2012) Reducing the impact of myocardial ischaemia/reperfusion injury. *Cardiovasc Res* 94:165–7

Plopper GE, McNamee HP, Dike LE *et al.* (1995) Convergence of integrin and growth factor receptor signaling pathways within the focal adhesion complex. *Mol Biol Cell* 6:1349–65

Romashkova JA, Makarov SS (1999) NF-kappaB is a target of AKT in anti-apoptotic PDGF signalling. *Nature* 401:86–90

Roy DC, Mooney NA, Raeman CH *et al.* (2013) Fibronectin matrix mimetics promote full-thickness wound repair in diabetic mice. *Tissue Eng*. online www.ncbi.nlm.nih.gov/pubmed/23808793

Sakai T, Johnson KJ, Murozono M *et al.* (2001) Plasma fibronectin supports neuronal survival and reduces brain injury following transient focal cerebral ischemia but is not essential for skin-wound healing and hemostasis. *Nat Med* 7:324–30

Saoncella S, Echtermeyer F, Denhez F *et al.* (1999) Syndecan-4 signals cooperatively with integrins in a Rho-dependent manner in the assembly of focal adhesions and actin stress fibers. *Proc Natl Acad Sci USA* 96:2805–10

Shupp JW, Nasabzadeh TJ, Rosenthal DS *et al.* (2010) A review of the local pathophysiologic bases of burn wound progression. *J Burn Care Res* 31:849–73

Singer AJ, Taira BR, Lin F *et al.* (2011) Curcumin reduces injury progression in a rat comb burn model. *J Burn Care Res* 32:135–42

Urano F, Wang X, Bertolotti A *et al.* (2000) Coupling of stress in the ER to activation of JNK protein kinases by transmembrane protein kinase IRE1. *Science* 287:664–6

Verma G, Datta M (2012) The critical role of JNK in the ER-mitochondrial crosstalk during apoptotic cell death. *J Cell Physiol* 227:1791–5

Wang J, Milner R (2006) Fibronectin promotes brain capillary endothelial cell survival and proliferation through alpha5beta1 and alphavbeta3 integrins *via* MAP kinase signalling. *J Neurochem* 96:148–59

Wang R, Clark RA, Mosher DF *et al.* (2005) Fibronectin's central cell-binding domain supports focal adhesion formation and Rho signal transduction. *J Biol Chem.* 280:28803–10

Wijelath ES, Rahman S, Namekata M *et al.* (2006) Heparin-II domain of fibronectin is a vascular endothelial growth factor-binding domain: enhancement of VEGF biological activity by a singular growth factor/matrix protein synergism. *Circ Res* 99:853–60

Yamada K.M, Clark RAF (1996) Provisional matrix. In: Clark RAF, ed *Molecular and Cellular Biology of Wound Repair*. Plenum Press: New York, NY, USA, 51–93

Yi M, Ruoslahti E (2001) A fibronectin fragment inhibits tumor growth, angiogenesis, and metastasis. *Proc Natl Acad Sci USA* 98:620–4

Yuan J (2009) Neuroprotective strategies targeting apoptotic and necrotic cell death for stroke. *Apoptosis* 14:469–77

Zhang Z, Vuori K, Reed JC *et al.* (1995) The alpha 5 beta 1 integrin supports survival of cells on fibronectin and up-regulates Bcl-2 expression. *Proc Natl Acad Sci USA* 92:6161–5